

Nov 3rd, 12:00 AM

Arc-spot Welds for Multi-overlap Roof Deck Panels

N. Guenfoud

R. Tremblay

C. A. Rogers

Follow this and additional works at: <https://scholarsmine.mst.edu/isccss>



Part of the [Structural Engineering Commons](#)

Recommended Citation

Guenfoud, N.; Tremblay, R.; and Rogers, C. A., "Arc-spot Welds for Multi-overlap Roof Deck Panels" (2010). *International Specialty Conference on Cold-Formed Steel Structures. 2.* <https://scholarsmine.mst.edu/isccss/20iccfss/20iccfss-session11/2>

This Article - Conference proceedings is brought to you for free and open access by Scholars' Mine. It has been accepted for inclusion in International Specialty Conference on Cold-Formed Steel Structures by an authorized administrator of Scholars' Mine. This work is protected by U. S. Copyright Law. Unauthorized use including reproduction for redistribution requires the permission of the copyright holder. For more information, please contact scholarsmine@mst.edu.

Arc-Spot Welds for Multi-Overlap Roof Deck Panels

N. Guenfoud¹, R. Tremblay², and C.A. Rogers³

Abstract

Roof deck construction often incorporates cold-formed steel panels that are connected to the underlying framing with the use of arc-spot welds. The welds are commonly located in areas where multiple layers of roof deck exist, such as at sidelaps or endlaps. CSA S136 restricts the use of multi-layer connections to being less than 2.5 mm thick; as well, the thickness of the supporting steel must exceed 2.5 times the aggregate thickness of the deck. In effect, the standard does not allow for the use of arc-spot welds for 18 ga (1.21 mm) and 16 ga (1.52 mm) roof deck panels. Nonetheless, it is not unusual for these deck panels to be used in construction; a solution to the arc-spot weld restrictions and a new welding protocol was needed. This situation led to the initiation of a research program on the shear resistance and tension resistance of multi-layer arc spot welds. The paper describes the welding protocol that was developed to obtain adequate quality and size arc-spot welds in up to four layers of 16 ga. deck. Weld test specimens were fabricated through one, two or four layers of steel sheets with thicknesses ranging from 22 ga. (0.76 mm) to 16 ga. (1.52 mm). Various sheet steel / weld configurations found in roof deck construction were included. A total of 72 tension tests and 107 shear tests were completed. Adequate weld quality could be achieved in all cases except that welds were undersized when the total sheet thickness becomes twice as large as the thickness of the underlying material. The results were compared with the current provisions of CSA S136 and modifications to the existing design equations are recommended.

¹ Graduate Student, Department of Civil, Geological and Mining Engineering, École Polytechnique, Montreal QC, Canada.

² Professor, Canada Research Chair in Earthquake Engineering, Department of Civil, Geological and Mining Engineering, École Polytechnique, Montreal QC, Canada.

³ Associate Professor, Department of Civil Engineering & Applied Mechanics, McGill University, Montreal QC, Canada.

Introduction

In North America roof deck diaphragms are commonly used as part of the lateral load resisting system. These diaphragms are composed of corrugated steel panels that may be connected to the underlying structure by arc-spot welds. Due to uplift actions caused by wind loads the welded connections must also resist tension forces. At the perimeter of each panel, the sidelap and endlap fasteners connect adjacent panels to the structure; this can result in connections comprising two and four layers of deck (Fig. 1).

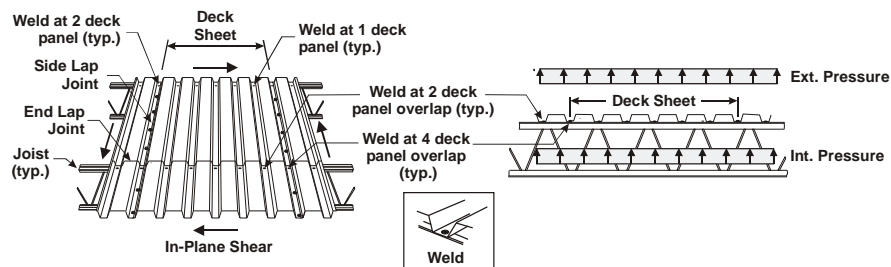


Figure 1: Steel deck panel connections and loading

CSA S136 (2007) contains provisions to determine the shear resistance and tensile resistance of arc-spot welds. These provisions, mainly based on tests that were carried out using thin deck (22 & 20 ga. (0.76 mm & 0.91 mm)), can be traced to the work of Peköz & McGuire (1979) and LaBoube & Yu (1991). CSA S136 limits the total thickness of sheet steel (deck thickness times the number of deck layers) for an arc spot weld connection to 3.81 mm. Section E2.2a of Appendix B (Canada) states that the maximum single sheet thickness shall be 2.0 mm and that the maximum aggregate sheet thickness of double sheets shall be 2.5 mm. The thickness of the supporting member must be at least 2.5 times the aggregate steel sheet thickness. Furthermore, the 2005 NBCC (NRCC, 2005) and CSA S16 (2001) necessitate the use of a capacity based seismic design approach which requires the roof deck diaphragm to have a shear resistance greater than the probable resistance of the vertical bracing system (Rogers & Tremblay, 2010). Consequently, the use of 18 (1.21 mm) and 16 ga. (1.52 mm) deck has become more common as stronger diaphragms are required.

Snow & Easterling (2008) performed shear tests on single, double and four-layer arc-spot weld connections for deck ranging from 0.76 mm to 1.52 mm. These deck-to-frame connections were fabricated using a shielded metal arc welding (SMAW) procedure that involved an E4310 (E6010) electrode. It was concluded that arc-spot welds can be adequately fabricated in single and double layers of sheet steel if the total thickness does not exceed 3.81 mm. It was also reported

that welds with sufficient penetration could not be fabricated in four layers of sheet steel. The 3.81 mm limit is exceeded when 16 and 18 ga. deck panels in the four layer sidelap/endlap configuration are required.

This research was initiated due to the lack of Canadian design information for arc-spot weld connections for the thicker deck panels. The scope of research was set to address the performance of multi-layer connections. The objective was to first identify a procedure that could be used to weld the connections, and to then verify if the current design provisions in CSA S136 for arc-spot welds are applicable to these thick deck sheet assemblies. The scope of research involved the testing of arc-spot weld connections fabricated through one, two or four layers of steel sheets with thicknesses ranging from 22 ga. (0.76 mm) to 16 ga. (1.52 mm). The findings of this research project are summarized herein; details on the test program can be found in Guenfoud *et al.* (2010).

Experimental Program

Welding Protocol and Procedure

In collaboration with a welding engineer and experienced certified welders a SMAW procedure for multi-overlap deck connections was first established; the key parameters affecting weld quality were identified as being the electrode type, the current setting and the welding technique. E4311 (E6011) electrodes were selected because they provided better penetration than other commonly used electrodes as observed by Peuler *et al.* (2002). Preliminary welding sessions were organized to verify the quality of welds fabricated and to refine the welding procedure. The final parameters used for the fabrication of the test specimens were: a) Circular welds having a visible diameter from 16 mm to 19 mm, b) 3.2 mm (1/8 in.) diameter E4311 (E6011) electrodes, and c) AC current set at 195 A when welding 16 and 18 ga. steel sheets, and 160 A when welding 20 and 22 ga. steel sheets. The welding procedure, similar to that elaborated by Peuler (2002), was selected because it facilitated piercing through thicker sheets while minimizing porosity. The weld was performed in the flat position. Once the arc was sparked, the electrode was pushed down vertically through the material to drill through the sheets until proper fusion of the underlying hot rolled steel was obtained. The electrode was then gradually withdrawn with a circular motion to allow the hole to be filled with molten metal. The arc was then broken vertically. The proposed settings represent laboratory conditions; field conditions might use this as a starting point but the final choice for optimum methods can vary depending on ambient conditions, welding equipment and the preferences of the welder.

Test Specimens and Set-up

The test program (Fig. 2) involved the two loading conditions encountered in roof deck construction, *i.e.* in-plane shear due to lateral loads and tension due to uplift wind pressure. Shear and tension connection test specimens were fabricated using four nominal sheet steel thicknesses: 0.76, 0.91, 1.21 and 1.52 mm. All specimens were made from galvanized ASTM A653 SS230 sheet steel with zinc thickness corresponding to Z275 (275 g/m², total of two faces).

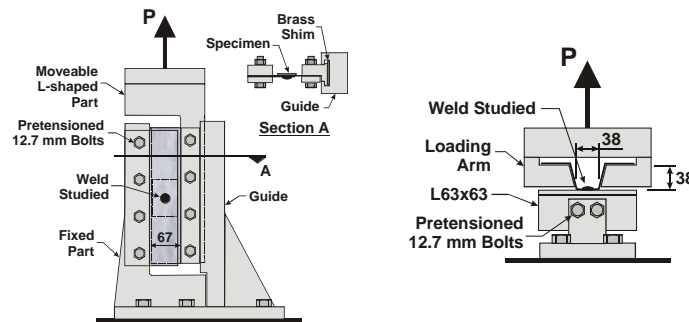


Figure 2: Steel deck panel shear and tension test set-up

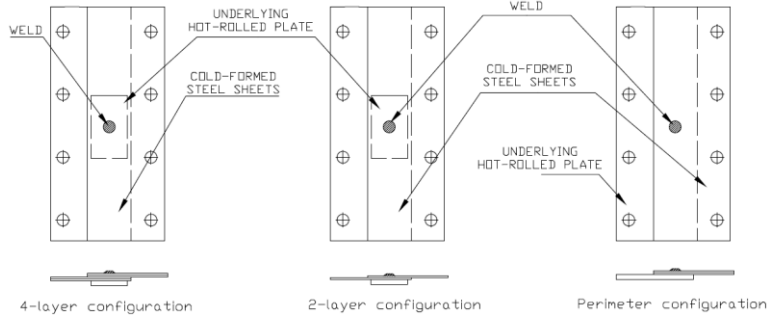


Figure 3: Steel deck panel shear test specimens

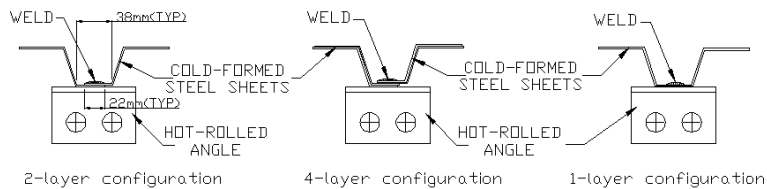


Figure 4: Steel deck panel tension test specimens

The shear specimens were made of two 102 x 280 mm overlapped steel sheets connected by a single weld (Fig. 3). To represent the underlying joist top chord or beam top flange, a 51 mm x 76 mm plate with thicknesses of 6.4 mm and 3.2 mm was used. These plates were made of CSA G40.21-350W steel with a one-coat primer. The set-up used to test the tension strength of the arc-spot welds was similar to that developed by LaBoube & Yu (1991). Steel sheets (100 mm long) were cut and cold bent to model one flute from the common 38 mm deep x 914 mm wide trapezoidal deck profile with flutes spaced 152 mm o/c (Fig. 4). At the bottom flange of the simulated flute, the sheets were welded to hot rolled CSA G40.21-350W steel L63x63 angles (one-coat primer) with thicknesses of 6.4 mm (1/4") and 3.2 mm (1/8") representing typical steel joist top chords.

Loading and Displacement Protocols

A monotonic loading protocol was used for all tension tests and 76 shear tests. The remaining 31 shear tests were carried out using a reversed cyclic loading protocol. Prior to running the cyclic tests, the data from the monotonic shear tests were compiled to provide an estimate of the average ultimate shear strength ($P_{u,avg.}$) for each connection configuration from which a loading protocol specific to each configuration was then determined.

Test Matrix

A listing of the connection test configurations is provided in Table 1. The first letter of the specimen number relates to the loading (M = monotonic, C = cyclic, and T = tension), "xx" is the gauge, followed by the number of plies, and "z" is the specimen number in a series. The letter "P" or "T" is added to identify the shear specimens at the perimeter of the diaphragm and when the thinner (3.2 mm) underlying material is used, respectively. The number of specimens is associated with a letter that gives the observed failure mode, as discussed below.

Test Results

Failure Modes

Three different failure modes were observed during the shear tests: weld shear failure (W), sheet tearing failure (T) and sheet bearing failure (B). Weld shear failure is characterized by fracture of the specimen through the weld nugget. Small displacements, a sudden loss in resistance and overall brittle behaviour are associated with this failure mode. Weld shear occurs mainly for the configurations that have a low weld diameter to total thickness ratio. When the effective diameter is relatively small compared to the thickness of the sheet steel

the critical load causing failure through the weld plane is reached before the sheet steel can exhibit significant deformations. When sheet tearing occurs (high d/t ratios), the failure initiates on the tension side of the weld and then spreads on a line perpendicular to the applied load. Out-of-plane deformations occur in the sheet steel on the compression side of the weld. Sheet bearing failure is characterized by piling of the steel in front of the weld nugget and by shearing of the sheet around the contour of the weld on lines parallel to the applied load.

During tension strength tests, two failure modes were encountered: weld failure (W) and sheet tearing failure (T). Weld failure, associated with small displacements, occurred for configurations with low d/t ratios. Sheet tearing is characterized by tearing of the sheet steel along the contour of the weld. A peeling effect caused by the geometry of the overlap connection was also observed.

Table 1 Test matrix and observed failure modes¹

Specimen No.	Sheet thickness (mm) / Gauge			
	0.76 / 22	0.91 / 20	1.21 / 18	1.52 / 16
Mxx2z	4T	4T	4T	4B
Mxx4z	2W+1T+1B	2W+1T+1B	4W	4W
Mxx2zP	2W+2T	1W+3T	4W	4W
Mxx2zT	4T	3T	4T	3W
Mxx4zT	2W+1T+1B	1W+1T+2B	3W	3W
Cxx2z	4T	4T	4T	4B
Cxx4z	1W+1T+2B	1W+1T+2B	3W	4W
Txx1z	3T	4T	4T	4T
Txx2z	4T	4T	4T	3W+1T
Txx4z	3T	1W+3T	1W+3T	3W
Txx2zT	5T	3T	3W	3T
Txx4zT	4T	1W+2T	3W	3W

¹Note: W = Weld failure, T = Sheet tearing failure, B = Bearing failure.

Effective Weld Diameter

In CSA 136 the resistance of welds subject to shear or tension is related to the effective weld diameter, d_{eff} . The cross-section of the weld nugget typically has a conical shape and, therefore, the diameter of the weld decreases over its depth. The visual weld diameter, d_{vis} , is measured at the surface of the weld whereas d_{eff} is located at the failure plane of the weld. The effective weld diameter is measured along the mid-thickness of the steel sheets for the four- and two-ply

shear specimens. Conversely, d_{eff} is at the interface between the cold-formed steel sheets and the hot rolled steel for the two-ply shear specimens representing an end lap connection to the perimeter beams and for the four-, two- and single-ply tension specimens. The difference between the visual diameter and the effective diameter increases as the total thickness of sheet steel above the expected failure plane, t , is increased:

$$d_{eff} = 0.7d_{vis} - 1.5t \leq 0.55d_{vis} \quad [E2.2.1.2-5] \quad (1)$$

The effective weld diameter was determined for all shear and tension specimens where weld failure occurred. A measure of pitting and porosity was deducted from the effective gross weld area to calculate the effective net weld area, A_{ne} , which was then used to obtain d_{eff} :

$$d_{eff} = \sqrt{4A_{ne} / \pi} \quad (2)$$

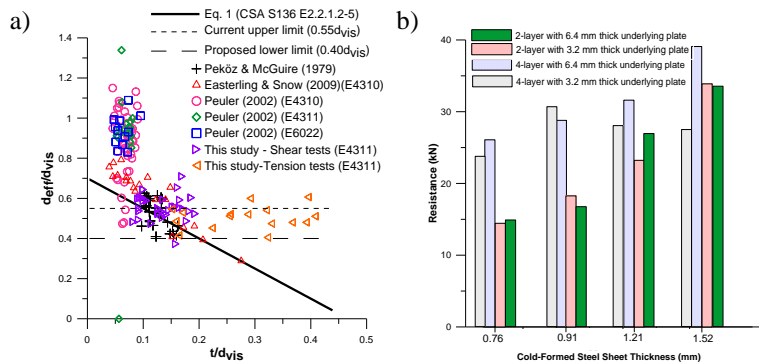


Figure 5 a) Effective weld diameter results; b) Influence of the thickness of the underlying plate on the shear strength of two-ply and four-ply specimens

Equation 1 has previously been found to be conservative because the measured effective weld diameters by Peuler (2002) were on average 50% higher than predicted. More recently, Snow & Easterling measured effective weld diameters that were on average 30% higher than those calculated using Eq. 1. It must be noted that the values published by Peuler as well as Snow & Easterling did not include a reduction to account for the porosity of the welds. A plot of the data recorded from the shear and tension specimens of this test program and the data reported from previous studies by Peköz & McGuire, Peuler and Snow & Easterling is provided in Fig. 5a. Specimens with “full-time welds” were plotted for the study by Snow & Easterling, the time spent making “full-time welds” being the minimum time

required to produce visual, average and effective diameters consistent with the dimensions required by the 2001 AISI Specification (AISI 2001). The measured values of d_{vis} were used to plot the data from this study.

The results show that Eq. E2.2.1.2-5 of CSA S136 accurately predicts d_{eff} for the t/d_{vis} range where tests had previously been carried out. This study also provided data in a t/d_{vis} range where few tests had previously been done. Figure 5a shows that Eq. E2.2.1.2-5 becomes overly conservative as t/d increases; a lower limit should be added if welds are fabricated with a welding procedure using an E4311 (E6011) penetrating electrode:

$$d_{eff} = 0.7d_{vis} - 1.5t, \text{ with } 0.4d_{vis} \leq d_{eff} \leq 0.55d_{vis} \quad (3)$$

Influence of the Thickness of the Underlying Framing Material

The failure modes and ultimate resistance of the shear and tension specimens fabricated with 3.2 mm and 6.4 mm framing material were compared. For the shear specimens, the failure mode was not influenced by the plate thickness. For two-layer specimens, the strength was found not to be affected by the thickness of the supporting material, regardless of the sheet thickness (Fig. 5b). The same holds true for the four-layer connections made with 22 to 18 ga. steel sheets. However, for the 4-layer specimens fabricated with 16 ga. (1.52 mm) material and 3.2 mm thick plates, the average measured shear resistance was 32% lower than the average measured shear resistance of the 4-layer specimens with 6.4 mm thick plates (Fig. 5b). The measured d_{vis} and d_{eff} were respectively 13% and 28% lower for specimens fabricated with 3.2 mm thick plates. These results show that when the plate material to total sheet steel thickness ratio is less than 0.5 the welder may experience more difficulty in producing welds with consistent effective weld diameters, which can result in reduced and more variable connection strength. No shear strength reduction was observed when the plate material to total sheet steel thickness ratio was equal to or greater than 0.7 (four 1.21 mm thick sheets on 3.2 mm plate), which is significantly less than the current minimum value of 2.5 specified in Appendix B of CSA S136.

The thickness of the angle had no influence on the behaviour and strength of the tension specimens fabricated with 22 and 20 ga. steel sheets. For specimens with 18 and 16 ga. steel sheets, a decrease in resistance was observed when 3.2 mm thick angles were used. It was observed that the angles deformed upon loading, causing stress concentrations along the perimeter of the weld thereby reducing the tension resistance of the weld. Such deformations did not occur with the 6.4 mm thick angles. In OWSJs the local flexibility of top chord angles will depend on several factors such as the angle size, the spacing and the stiffness of the joist

web members, etc., and it is therefore not possible to prevent angle deformations on the sole basis of a minimum angle to total sheet thickness ratio. Further research is needed to properly address this issue. In the test specimens, however, the average measured visible weld diameter of the 18 and 16 ga. steel sheet specimens with 3.2 mm thick angles was 17% smaller than for specimens fabricated with thicker underlying angles, leading to a smaller effective weld size and reduced capacity, similar to the shear tests. For the 4-layer specimens with 3.2 mm thick angles, the average measured A_{ne} of 16 ga. specimens was 20% less than that of the specimens composed of 18 ga. steel sheets. As such, welders may experience difficulty producing quality welds through 4 layers of 16 ga. (1.52 mm) steel sheet if the angle does not provide an adequate heat sink.

Analysis of CSA S136 Shear Resistance Equations

The results of the 76 monotonic shear tests were used to validate the CSA S136 equations. In tests with weld fracture, the resistance of the specimen is governed by the effective diameter of the weld. For sheet failure, the thickness of the steel sheets above the plane of maximum shear, and the visible weld diameter influence the shear strength. When considering the 33 shear tests with weld failure, the comparison of the measured effective weld diameter with the values predicted by Eq. E2.2.1.2-5 from CSA S136 provided an average test-to-predicted ratio of 1.13 with a coefficient of variation of 0.15. Equation E2.2.1.2-5 accurately predicts the d_{eff} for the range of t/d_{vis} corresponding to the shear specimens ($0.06 < t/d_{vis} < 0.2$). Equation 4 is used to evaluate the resistance of the connection specimens with regard to the weld shear failure mode:

$$P_u = \frac{\pi d_{eff}^2}{4} 0.75 F_{xx} \quad [E2.2.1.2-1] \quad (4)$$

Using the nominal tensile strength of the weld metal ($F_{xx} = 430$ MPa) and the measured d_{eff} , the average test-to-predicted resistance ratio for the shear specimens that failed due to weld fracture is 1.42 with a coefficient of variation of 0.15. This trend is consistent with that obtained by Peköz & McGuire who reported an average test-to-predicted ratio of 1.22 with a coefficient of variation of 0.30 for similar tests. The relationship between P_u and Eq. E2.2.1.2-1 is plotted in Fig. 6. The comparison shows that Eq. 4 consistently under-predicts the shear resistance of welded connections for the range of d_{eff} examined. This is likely caused by the difference between the actual and nominal values of the tensile strength of the weld metal. It is difficult to measure F_{xx} of the weld metal as it can vary significantly over the weld failure plane. The results show that Eq. E2.2.1.2-1 can safely be used to determine the shear resistance for arc spot weld failures in multi-overlap configurations.

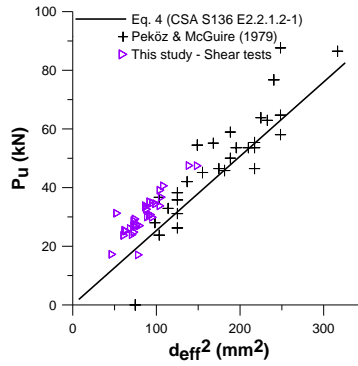


Figure 6 Relationship between P_u and d_{eff}^2 of CSA S136 Eq. E2.2.1.2-1

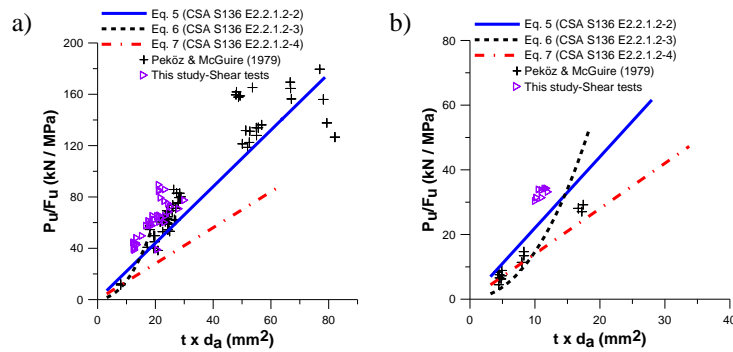


Figure 7 Relationship between measured arc spot weld shear strength and $t \times d_a$ for: a) Bearing failure; b) Tearing failure

Equations E2.2.1.2-2 to E2.2.1.2-4 in CSA 136 are used to predict the shear strength when shear failure occurs in the sheet material:

$$\text{for } (d_a / t) \leq 0.815 \sqrt{E / F_u} : \\ P_u = 2.20 t d_a F_u \quad [E2.2.1.2-2] \quad (5)$$

$$\text{for } 0.815 \sqrt{E / F_u} < (d_a / t) < 1.397 \sqrt{E / F_u} : \\ P_u = 0.280 \left[1 + 5.59 \frac{\sqrt{E / F_u}}{d_a / t} \right] t d_a F_u \quad [E2.2.1.2-3] \quad (6)$$

$$\text{for } (d_a / t) \geq 1.397 \sqrt{E / F_u} : \\ P_u = 1.40 t d_a F_u \quad [E2.2.1.2-4] \quad (7)$$

In these equations, $d_a = d_{vis} - t$, where t is the thickness of steel above the plane of maximum shear in the weld, *i.e.* the plane where d_{eff} was measured for the specimen with weld failure, and F_u is the tensile strength of the steel sheet. The test data was compared to the predicted values using the measured values of d_{vis} and F_u . Of all monotonic shear specimens, 35 were governed by Eq. 5. This equation is associated with a bearing failure mode. In Fig. 7a, Eqs. 5 to 7 are plotted with the test results and the data by Peköz & McGuire.

A trend can be observed where the measured resistance is generally higher than the predicted resistance. The average test-to-predicted resistance ratio was 1.44 with a coefficient of variation of 0.14 for the group of specimens tested in this experimental program. Likewise, Peköz & McGuire reported an average test-to-predicted resistance ratio of 1.15 with a coefficient of variation of 0.17 while Snow & Easterling reported a ratio of 1.28 with a coefficient of variation of 0.09 for similar specimens. The difference between the three ratios may be attributed to differences in weld quality. Although this data was not recorded, some specimens may not have had efficient connectivity along the entire perimeter of the weld, which would inevitably lower the resistance of the specimen. When analysing the data collected during this experimental program the best fit formula to replace equation E2.2.1.2-2 was found to be:

$$P_u = 2.40td_aF_u, \text{ for } (d_a/t) \leq 0.815\sqrt{E/F_u} : \quad (8)$$

This proposed equation was analyzed in accordance with Section F.1 of CSA S136 which specifies the statistical treatment to determine the structural performance for limit states design. The average test-to-predicted ratio was 1.32 with a coefficient of variation of 0.14. A reliability index of 4.0 can be attained with a resistance factor $\phi = 0.6$.

A total of 8 specimens were governed by Eq. 6 because of the d_a/t range. The average test-to-predicted resistance ratio for specimens governed by this equation is 1.58 with a coefficient of variation of 0.04. The data measured in this study and the data by Peköz & McGuire are compared to the predicted values in Fig. 7b. Equation 6 generally underestimates the resistance of the tested specimens. However, too few specimens were governed by this equation during this test program to warrant the modification of the current CSA S136 equation. Based on the available test data, it seems that Eq. 6 can safely be used to predict the shear resistance of specimens with multi-overlap configurations when $0.815\sqrt{E/F_u} < (d_a/t) < 1.397\sqrt{E/F_u}$. Further research targeting this specific range of specimens should however be carried out to validate the accuracy of Eq. E2.2.1.2-3. Of all the specimens tested during this experimental

program, none presented a d_a/t ratio indicating that Eq. E2.2.1.2-4 would govern, hence no conclusions have been drawn regarding its accuracy.

Analysis of CSA S136 Tension Resistance Equations

The results showed that when the specimen behaviour was governed by weld fracture d_{eff} influenced the tension resistance. When the tension specimens were governed by sheet failure, the total thickness of sheet steel above the underlying material and the average weld diameter influenced the tension resistance. As discussed, the thickness of the underlying joist angle also influenced the resistance of the specimens as thinner supporting material can distort upon loading and create stress concentrations that can adversely affect the resistance of the specimen. The deformation of the support can be avoided by using hot rolled angles with a minimum thickness of 6.4 mm. Section E2.2.2 of CSA S136 is used by designers to determine the tensile resistance of arc-spot welds:

$$P_u = \frac{\pi d_{eff}^2}{4} F_{xx} \quad [E2.2.2-1] \quad (9)$$

$$P_u = 0.8 \left(F_u / F_y \right)^2 t d_a F_u \quad [E2.2.2-2] \quad (10)$$

Equation 9 is related to weld failure in tension whereas Eq. 10 addresses the sheet tearing failure mode. CSA S136 specifies a 30% reduction for welds fabricated in sidelap joints. This reduction applies to sheet tearing when part of the weld connects to the overlapped sheet; this was not the case as the unstiffened flange width was larger than the visible weld diameter in all tests.

A total of 16 tension specimens failed due to weld fracture. The majority of these specimens (14) were fabricated with 1.21 and 1.52 mm thick steel sheets, the remaining two being made with 0.91 mm sheets. The resistance of such specimens is related to the effective weld diameter of each specimen. Figure 8a contains a plot of Eq. 9 without the 30% reduction in resistance. The data set is divided into two groups: 9 specimens where bending of the underlying angle was observed (3.2 mm thick angle with 18 ga. and thicker sheets) and 7 specimens where bending of the angles was not observed (6.4 mm thick angle or 20 ga. and thinner sheet steels). Test data for weld failure in tension reported by LaBoube & Yu (1991) for 4 non sidelap connections are also shown. Good match is found between Eq. E2.2.2-1 and the test data by LaBoube & Yu. The data produced in this test program is generally lower, with average test-to-predicted ratios of 0.50 and 0.56 for the entire data set and the subset where angle bending was not observed, respectively. Test specimens by LaBoube &

Yu had smaller effective diameters and washers were used in the welds, which favoured uniform stress distribution over the weld area. In this test program, the larger effective weld diameters and the absence of washer likely led to tensile stress concentrations along the perimeter of the welds, resulting in lower capacities; this phenomenon was probably accentuated when bending of the angle legs occurred. Considering that steel joists with thin angles are not uncommon in practice, it is proposed that Eq. 9 [E2.2.2-1] be modified based on the entire test data set by introducing a reduction factor of 0.5:

$$P_u = \frac{\pi d_{eff}^2}{4} 0.5 F_{xx} \quad (11)$$

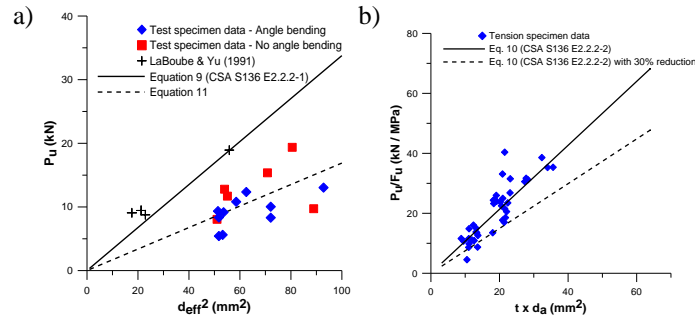


Figure 8 Relationship between measured arc spot weld tension strength and: a) d_{eff}^2 for weld failure; b) $t \times d_a$ for sheet tearing failure.

Using Eq. 11 (Fig. 8a), the average test-to-predicted ratio is equal to 1.0 with a coefficient of variation of 0.27; the resistance factor must be lowered to 0.32 to attain a reliability index of 4.0. If only the subset of 7 specimens for which angle bending was not observed is considered, a reduction factor of 0.56 is needed to achieve a test-to-predicted ratio of 1.0. The coefficient of variation is then equal to 0.26 and a resistance factor of 0.29 is required to obtain a reliability index of 4.0. In practice, Eq. [E2.2.2-1] will be used with effective diameter values obtained from Eq. (3). In this equation, the total thickness of sheet steel was used as the failure plane was located between the steel sheets and the steel angle. On average over the 16 test specimens, the so-computed effective weld diameter from Eq. 3 was equal to 1.22 times the measured effective diameters.

A total of 40 tension specimens with 2-layer and 4-layer configurations failed due to sheet failure. Equation 10 predicts the tensile resistance of specimens when sheet failure is involved and Section E2.2.2 specifies that this resistance be

reduced by 30% for arc-spot welds fabricated in sidelap configurations. Figure 8b illustrates Eq. E2.2.2-2 with and without the 30% reduction in capacity. The results obtained during the testing program are also plotted in Fig. 8b as a function of the measured visible weld diameter determined with the sheet steel thickness equal to half of the total thickness as failure always occurred at the mid-thickness of the steel sheets. The test data indicates that the 30% reduction does not apply to the specimens examined in this study. LaBoube & Yu (1991) proposed the 30% reduction to account for the fact that the unstiffened flange width of their specimens was small compared to d_{vis} . Using the measured specimen properties and the non reduced resistance from Eq. E2.2.2-2, the average test-to-predicted resistance ratio is equal to 1.17 with a coefficient of variation of 0.28. On this basis, a resistance factor of 0.38 must be applied to attain the reliability index of 4.0.

Conclusions

The type of electrode (E4311 (E6011)), high current setting and proper welding technique affect the quality of arc-spot welds in multi-layer connections. A lower limit for the net effective weld diameter was proposed. The shear resistance of arc-spot welds that are governed by weld failure are influenced by the net effective diameter of the weld. For specimens that are governed by sheet failure the total thickness of the steel sheets and the average weld diameter influence the shear resistance of the specimen. The tests also revealed that the shear strength of arc spot welds was not reduced when the thickness of the underlying material to the total sheet thickness was greater than 0.7. The data obtained during the shear resistance tests showed that Eq. E2.2.1.2-2 (bearing failure) was generally conservative; as such a modification to the coefficient was proposed.

Tension test specimens governed by weld fracture are influenced by the net effective weld diameter of the weld. The thickness of the underlying joist angle can also influence the resistance of the specimens if the loading causes deformations in the support. The resistance of tension specimens governed by sheet failure is influenced by the total thickness of sheet steel and the average weld diameter.

When tension weld failure governs, the results indicate that a 50% reduction in capacity should be applied to the resistance obtained from Eq. E2.2.2-1. A resistance factor $\phi = 0.32$ is proposed. These recommendations should apply to all connections, including those made of single sheets, because there is no evidence to suggest that the multi-overlap configuration influences the resistance of specimens governed by this failure mode. Test data for tension

failure by sheet tearing suggests that a reduced resistance factor $\phi = 0.38$ should be used in Eq. E2.2.2-2.

Acknowledgements

The authors thank NSERC, the CSSBI and the SSEF for their support in sponsoring this project. Additionally, appreciation is extended to G. Trigo from Consultarc for his valuable contribution on welding procedures.

References

- AISI (2002) Cold-formed steel design manual, American Iron and Steel Institute, Washington, USA.
- AISI (2001) North American specification for the design of cold-formed steel structural members, 2001 Edition, With 2004 supplement, American Iron and Steel Institute, Washington, USA.
- CSA (2001) S16, Limit states design of steel structures, Canadian Standards Association, Toronto, Canada.
- CSA (2007) S136, North American specification for the design of cold-formed steel structural members, Canadian Standards Association, Toronto, Canada.
- Guenfoud, N., Tremblay, R., Rogers, C. (2010) Experimental program on the shear capacity and tension capacity of arc spot weld connections for multi-overlap roof deck panels, Rept. No. SR-10-01, Dept. of Civil, Geological, and Mining Eng., Ecole Polytechnique, Montreal, Canada.
- LaBoube, R.A., Yu, W.W. (1991) Tensile strength of welded connections, Final Rpt., Civil Eng. Studies 91-3, University of Missouri-Rolla, Rolla, USA.
- NRCC (2005) National building code of Canada 2005, 12th ed., National Research Council of Canada, Ottawa, Canada.
- Peköz, T., McGuire, W. (1979) Welding of sheet steel, Report SG-79-2, American Iron and Steel Institute, Washington, USA.
- Peuler, M. (2002) Inelastic response of arc-spot welded deck-to-frame connections for steel roof deck diaphragms, Project Report, Dept. of Civil Engineering and Applied Mechanics, McGill University, Montreal, Canada.
- Peuler, M., Rogers, C.A., Tremblay, R., (2002) Inelastic response of arc-spot welded deck-to-frame connections for steel roof deck diaphragms, Proc. 16th Int. Spec. Conf. on Cold-Formed Steel Struct., Orlando, USA, 763-778.
- Rogers, C.A., Tremblay, R. (2010) Impact of diaphragm behaviour on the seismic design of low-rise steel buildings, Eng. J., AISC. (in press)
- Snow, G.L., Easterling, W.S. (2008) Strength of arc-spot welds made in single and multiple steel sheets, Proc. 19th Int. Spec. Conf. on Cold-Formed Steel Struct., St. Louis, USA, 607-622.

